Microscopic evidence for Ca^{2+} mediated pectin-pectin interactions in carrot-based suspensions

Clare Kyomugasho, Katleen Willemsen, Stefanie Christiaens, Ann M. Van Loey and Marc E. Hendrickx*

Laboratory of Food Technology, Leuven Food Science and Nutrition Research Centre (LFoRCe), Department of Microbial and Molecular Systems (M^2S), KU Leuven, Kasteelpark Arenberg 22, Box 2457, 3001 Leuven, Belgium

*Corresponding author (telephone +32 16 321572; fax +32 16 321960; e-mail Marc.Hendrickx@biw.kuleuven.be).

Abstract

This study explored the use of fluorescently labeled pectin to obtain evidence for Ca^{2+} mediated pectin-pectin interactions *in situ*. Specifically, carrots were either blanched at low temperature (LTB) or blanched at high temperature (HTB) to activate or inactivate endogenous pectin methylesterase, respectively. Consequently, pectin in tissue particles of LTB and HTB carrots exhibited low degree of methylesterification (DM) and high DM, respectively. Pectin present in the LTB carrot serum exhibited a lower DM, was more branched, and showed a higher molar mass compared to HTB carrot serum pectin. Ca^{2+} mediated pectin-pectin interactions were influenced by serum pectin molecular structure, increased with increasing pH and Ca^{2+} concentration, and decreasing DM. Presence of more linear pectin in the serum created a competition, leading to less intense interactions between labeled pectin and pectin at tissue particle surfaces. Generally, the most intense Ca^{2+} mediated pectin-pectin interactions were observed for pectin of LTB carrot particles.

Keywords: Carrot; Degree of methylesterification; Ca^{2+} mediated pectin-pectin interactions; Labeled pectin.

1. Introduction

To increase shelf life, ease transportation and provide a variety of products to consumers, the edible portions of fruits and vegetables are more and more processed into high quality particulated products such as juices, purées and soups. During processing, mechanical disintegration techniques (such as crushing, blending and high-pressure homogenisation) are applied to obtain the fruit- and vegetable-derived particulated products. These types of products are commonly described as a combination of a liquid phase or serum containing salts, sugars, proteins, organic acids and pectic substances, and a dispersed phase consisting of all the plant insoluble solids, mainly cell wall material (Lopez-Sanchez et al., 2011). Pectin present in the serum phase and in the particle phase plays an important role in structural/rheological and functional properties of fruit- and vegetable-derived food products. Therefore, changes in pectin structure that may occur during processing will influence the functionality of pectin.

Pectin is a heterogeneous group of closely associated cell wall polysaccharides rich in galacturonic acid (GalA). Three pectic polysaccharides (homogalacturonan (HG), rhamnogalacturonan-I (RG-I) and rhamnogalacturonan-II (RG-II)) have been isolated from primary cell walls and structurally characterized (Ridley, O'Neill, & Mohnen, 2001; Houben, Jolie, Fraeye, Van Loey, & Hendrickx, 2011). These pectic polysaccharides are believed to be covalently linked to each other but also show interactions by non-covalent linkages such as Ca^{2+} cross-links, hydrogen bonds and hydrophobic interactions (Sanchez, 2011; Caffall & Mohnen, 2009). The HG polymer, which is the predominant pectic polysaccharide in the cell walls and middle lamella of plants consists of a backbone of α-1,4-linked GalA residues. The GalA moieties within the backbone of the HG pectic polymer may be methylesterified at C-6 and/or O-acetylated at O-2 and/or O-3 (Voragen, Coenen, Verhoef, & Schols, 2009; Sila et al., 2009). RG-

I on the other hand possesses a backbone of the repeating disaccharide [→4)-α-D-GalA-(1→2)-α-L-rhamnose-(1→], with a number of different side chains attached to the C-4 position of rhamnose, which are principally composed of L-arabinose and D-galactose. Lastly, RG-II consists of an HG backbone of seven to nine 1,4-linked GalA residues with four well defined side chains (two structurally distinct disaccharides and two structurally distinct oligosaccharides) (Ridley et al., 2001; Caffall & Mohnen, 2009). The degree of methylesterification of HG is a major factor determining pectin (Ca^{2+}) interactions which in turn determine pectin functionality. Reducing the degree of pectin methylesterification, for example, by activating endogenous pectin methylesterase (PME) activity which in this research was done by controlling environmental conditions (60 °C for 24 h), results in increased intercellular adhesion in plant tissue material (Fraeye et al., 2009). This behavior in plant cell walls can be mainly attributed to the ability of the demethylesterified pectin to interact with metal ions, particularly Ca^{2+}-ions, and the decreased susceptibility of the pectin to depolymerisation by β-elimination (Thakur, Singh, & Handa, 1997). In addition to the DM, the distribution of non-methylesterified GalA residues is also important in terms of pectin functionality/interactions with Ca^{2+}. For instance, blocks of more than ten non-methylesterified GalA residues yield pectin molecules that are sensitive to Ca^{2+} cross-linking (Voragen et al., 2009; McFeeters, 1985; Kim & Wicker, 2011). The more blockwise the distribution of free carboxyl groups, the higher the Ca^{2+} sensitivity (Sila et al., 2009). Furthermore, the strength of calcium binding increases as the DM decreases. However, even at high DM, pectin with a blocky distribution will form calcium gels. High DM pectin with high degree of blockiness will form calcium gels at lower calcium concentrations and give stronger gels compared to pectins with less blocky distribution (Strom et al., 2007; Lofgren & Hermansson, 2007; Strom, Lundin, Morris, & Williams, 2012). Ca^{2+} mediated pectin-pectin

cross-linking is greatly exploited commercially in gelation applications where, Ca^{2+} cross-linking of HG increases firmness by bringing blocks of non-methylesterified HG chains into a tightly packed conformation (Caffall & Mohnen, 2009; Brummell, 2006). Additionally, Ca^{2+}-mediated cross-linking has also been applied to preserve the texture of intact plant tissues upon processing (Fraeye et al., 2009). Furthermore, many Ca^{2+} mediated pectin-pectin interactions and functionalities of pectin are influenced by its neutral sugar and GalA composition (degree of branching/linearity), degree of polymerisation and degree of acetylation (Yapo, Lerouge, Thibault, & Ralet, 2007; Kim & Wicker, 2011). For example, depolymerisation of pectin is a major contributor to weakening of the middle lamella and declining intercellular adhesion in plant tissues, which in turn leads to loss of texture/firmness. Finally, extrinsic factors such as pH and calcium concentration also significantly influence Ca^{2+} mediated pectin-pectin interactions of pectin-based systems. For instance, in particulated fruit- and vegetable-based products, the carboxyl groups of pectin at the surface of tissue particles or in the liquid phase can be negatively charged (depending on the pH), leading to electrostatic interactions between the particles in presence of divalent ions such as Ca^{2+} (Moelants et al., 2014; Haghighi & Rezaei, 2012).

To study pectin interactions, a selective extraction of pectic fractions from cell wall material is commonly performed followed by a physicochemical analysis of the fractionated cell walls and isolated polymers (Christiaens et al., 2012). Recently, analytical techniques that are less time consuming and less invasive to the sample have been implemented for exploring these interactions. Furthermore, these new techniques eliminate the possibility of changes in pectin structure that may occur during its isolation from plant tissue (Sriamornsak, 2003). For instance, Christiaens et al. (2011), explored the use of anti-HG antibodies for assessment of the effect of

112 food processing on pectin in intact plant cell walls. In this research, the use of fluorescently
113 labeled pectin to gain insight into Ca^{2+} mediated pectin-pectin interactions in processed carrot
114 tissue suspensions is explored. Although some information pertaining to labeling of pectic
115 oligosaccharides and polysaccharides with fluorescent tags is available in literature, (Ishii, Ichita,
116 Matsue, Ono, & Maeda, 2002; Nordmark & Ziegler, 2000; Tromp, de Kruif, van Eijk, & Rolin,
117 2004), surprisingly these labeled carbohydrates have not yet been used in understanding pectin-
118 interactions in complex food systems. In addition, fluorescent labeling of pectins with different
119 DMs has not been performed so far. Therefore, this work is aimed at bridging this gap. In
120 particular, the interactions between fluorescently labeled exogenous pectins (with different DMs)
121 and pectin of different DMs created at the surface of the tissue particles or in the liquid phase of
122 carrot suspensions through selective processing are investigated. Using fluorescence microscopy,
123 the extent of Ca^{2+} mediated pectin-pectin cross-linking can be evaluated by examining the tissue
124 particle surfaces and/or liquid phase for fluorescence induced by the labeled pectin. Carrot
125 suspensions were particularly selected as a study subject due to the fact that carrot is a low acid
126 vegetable in which PME-induced pectin changes, and thus Ca^{2+} mediated pectin-pectin
127 interactions, play an important role in pectin functionality.

128 ## 2. Materials and Methods

129 ### 2.1 Production of carrot purées

130 Fresh yellow carrots (*Daucus carota* cultivar Yellow Mellow) from a local supplier in Belgium
131 (stored for up to two days at 4 °C) were peeled and cut into one cm^3 pieces. The cubes were
132 vacuum sealed in polyethylene bags and either blanched at high temperature (5 min, 95 °C), to
133 inactive the endogenous enzymes, or incubated at 60 °C for 24 h to allow action of endogenous

PME, after which, a blanching step followed (5 min, 95 °C) to inactivate all the endogenous enzymes. The samples were rapidly cooled in an ice bath, frozen with liquid N_2 and stored at -80 °C. High temperature blanched samples were denoted as HTB while low temperature blanched samples were denoted as LTB. For further analysis, the samples were thawed at 25 °C, weighed, and an equal amount of demineralised water (w/w) was added. Purée was subsequently prepared from the samples by blending for 20 sec at low speed, followed by 40 sec at high speed in a blender (Magimix, Vincennes, France). HTB and LTB carrot purées were used in further sample preparation (see section 2.2 & 2.3).

2.2 Separation of carrot purée particles based on size

One part of each purée was separated into fractions with different particles sizes using the wet sieving technique. A sieve shaker (Retsch, Aartselaar, Belgium) equipped with a set of sieves with pores sizes of 40, 80, 125, 250, 500 and 1000 µm was used. Pulp obtained on each sieve was assembled and drained over a filter to remove excess water as described by Moelants et al. (2014). The particles obtained were either used for the isolation of alcohol insoluble residue for further pectin characterisation (see section 2.4) or stored over 70% ethanol for at least two weeks before further use for microscopy examinations (see section 2.7).

2.3 Extraction of the liquid phase (serum) from the purées

The remaining part of the purée was centrifuged (30 min, 20 °C and 12400 g) and the supernatant obtained was filtered (Machery-Nagel MN615 ϕ 90 mm) under vacuum to completely separate particles from the liquid phase (serum). A part of this serum was lyophilised and used for pectin characterisation while the remaining part was used for reconstituting carrot tissue particles for microscopy studies.

2.4 Characterisation of pectin

Cell wall material present in the particle fractions (obtained in section 2.2) was extracted as alcohol insoluble residue (AIR) and the DM of the AIR was determined. On the other hand, pectin present in the serum (obtained in section 2.3) was characterized for its DM, GalA content, neutral sugar composition and molar mass distribution.

2.4.1 Isolation of the alcohol insoluble residue

Cell wall material in tissue particle fractions was isolated as AIR using the method described by McFeeters & Armstrong (1984). Approximately 30 g of sample was homogenised in 192 mL of 95% ethanol using a mixer (Büchi mixer B-400, Flawil, Switzerland). The resulting suspension was filtered (Machery-Nagel MN615 ϕ 90 mm) and the residue obtained was rehomogenised in 96 mL of 95% ethanol. After a second filtration step, the resulting residue was homogenised in 96 mL of acetone. The final residue after the last filtration step was dried overnight at 40 °C to obtain the AIR, which was then stored over P_2O_5 in a desiccator until further use.

2.4.2 Determination of degree of methylesterification

The DM of pectin was determined using the FT-IR method described by Kyomugasho et al. (2015). Approximately 10 mg of AIR was dissolved in demineralised water and the suspension was adjusted to pH 6 with NaOH (0.1 N or 0.01 N). Serum samples on the other hand were directly adjusted to pH 6. The samples were transferred into Spectra/Por® dialysis tubing (3.5 kDa, molecular weight cut-off (MWCO)) and dialysed against demineralised water for 48 h. Afterwards, the samples were lyophilised and stored over P_2O_5. For DM determination, a small sample was firmly compacted to expel entrapped air and create smooth surfaces. This sample was then placed on the sample holder of the FT-IR (Shimadzu FTIR-8400S, Japan) and the

transmittance was measured at wave numbers from 4000 cm^{-1} to 400 cm^{-1} at resolution 4 cm^{-1}. To obtain a high signal to noise ratio, 100 scans were run per sample and integrated spectra mean values were collected. After spectra preprocessing, the absorption intensity of the bands situated around 1740 cm^{-1} (due to ester carbonyl group (C=O) stretching) and 1630-1600 cm^{-1} (due to carboxylate group (COO^-) stretching) (Szymanska-Chargot & Zdunek, 2013) were used to predict the DM. In particular, using the standard curve, Y= 123.45X + 6.9514, the DM (Y) was predicted from the ratio (X) of the band at 1740 cm^{-1} to the sum of the bands at 1740 cm^{-1} and 1630-1600 cm^{-1}. A high precision of DM measurement was obtained using this method as validated by Kyomugasho et al. (2015).

2.4.3 Determination of galacturonic acid content

The galacturonic acid (GalA) content of carrot serum pectin was determined based on the method described by Ahmed and Labavitch (1977). The pectin material was hydrolysed (in duplicate) with concentrated sulfuric acid and was subsequently diluted with demineralised water. The GalA concentration was then analysed according to the spectrometric method of Blumenkrantz and Asboe-Hansen (1973). The analysis was performed in triplicate.

2.4.4 Neutral sugar analysis

The neutral sugar composition of the lyophilised serum samples was analysed using high-performance anion-exchange chromatography (HPAEC) combined with pulsed amperometric detection (PAD). Approximately 5 mg of sample was weighed into pyrex tubes and digested in 0.5 mL of 4 M trifluoroacetic acid (TFA) for 1.5 h at 110 °C in an oil bath. The digest was cooled, transferred into specific glass tubes and dried at 45 °C under a N_2-evaporator (Techne FDB03DD, Cambridge, UK). Thereafter, the dried sample was washed with 0.25 mL of 1 M

200 NH_4OH to remove/neutralize TFA and dried again under N_2 at 45 °C. The residue obtained after
201 the second drying was dissolved in ultrapure water (organic free, 18.2 MΩ cm resistance),
202 filtered through a 0.45 µm filter (Chromafil® A-45/25, German) and injected onto the HPAEC-
203 PAD. After equilibration with 100 mM NaOH for 5 min followed by equilibration with 4 mM
204 for 5 min, 10 µL of sample was injected and isocratically eluted for 20 min with 4 mM NaOH at
205 a flow rate of 0.5 mL/min and 30 °C. To detect and quantify the monosaccharides, potentials of
206 E_1 = 0.1 V, E_2 = -2.0 V, E_3 = 0.6 V and E_4 = -0.1 V were held for duration times t_1 = 400 ms, t_2
207 + t_3 = 40 ms and t_4 = 60 ms respectively. Mixtures of available sugar standards (L-fucose, L-
208 rhamnose, L-arabinose, D-galactose, D-glucose, D-xylose, D-mannose and galacturonic acid) at
209 varying concentrations (1-10 ppm) were used as external standards for identification and
210 quantification. All samples were analysed in duplicate. To correct for degradation of
211 monosaccharides during the acid hydrolysis step, recovery values were estimated. Hetero
212 mixtures of sugar standards were also subjected to hydrolysis conditions (hydrolysed standard
213 samples) and the peak areas were compared to those of non-hydrolysed standard mixtures
214 (Houben et al., 2011).

215 2.4.5 Molar mass distribution

216 The molar mass distribution of serum pectin was estimated using high-performance size-
217 exclusion chromatography equipped with multi-angle laser light scattering (PN3621, Postnova
218 analytics, Germany) and refractive index (RI) detection (Shodex RI-101, Showa Denko K.K.,
219 Kawazaki, Japan). Approximately 5 mg of serum sample was weighed and dissolved in 4 mL of
220 filtered buffer (0.1 µm) of pH 6.3 (0.1 M 2-morphlinoethanesulfonic acid (MES monohydrate)
221 containing 0.1 M NaCl). The dissolved samples were filtered through 0.45 µm syringe filters
222 (Chromafil® A-45/25, German) before injection. An aliquot of the sample (100 µL) was then

injected onto a series of Waters columns (Waters, Milford, MA), i.e., Ultrahydrogel 250, 1000, and 2000 with exclusion limits of $8*10^4$, $4*10^6$, and $1*10^7$ g/mol, respectively, and eluted with the NaCl containing MES monohydrate buffer at 35 °C with a flow rate of 0.5 mL/min. The eluent was monitored with an RI detector and a MALLS detector. Each sample was analysed in duplicate and the molar masses were calculated using the Debye fitting method (2^{nd} order) of the operating software (Nova Mals, version 1.0.0.18, Postnova analytics) provided by the manufacturer of the MALLS detector as described by Shpigelman et al. (2014).

2.5 Immunolabeling of pectin at the surface of carrot tissue particles

Presence of pectin at the surface of carrot tissue particles was established through immunolabeling as described by Christiaens et al. (2011). Three monoclonal primary antibodies (JIM7, PAM1 and 2F4) were used for characterisation and identification of pectin. For visualization, secondary labeling with an anti-rat Ig antibody (for JIM7) and an anti-mouse IgG antibody (for 2F4), coupled to fluorescein isothiocyanate (FITC) (Nordic immunology, Tilburg, Netherlands) was performed. In the case of PAM1, a three stage labeling was performed. After primary labeling, the sample was incubated with an anti-polyhistidine antibody (sigma-Aldrich, St. Louis, Missouri), followed by incubation with an anti-mouse IgG antibody coupled to FITC. JIM7 was used for recognition of pectin with a wide range in DM (stronger binding to high methylesterified pectin regions) while PAM1 was selected due to its specificity for blocks of non methylesterified GalA residues. 2F4 on the other hand recognizes regions of HG that are Ca^{2+} cross-linked (Christiaens et al., 2011).

2.6 Production of covalently labeled citrus pectins with different degrees of methylesterification

The production of covalently labeled citrus pectins with different DMs was achieved in three stages: (i) demethylesterification of pectin, (ii) oxidation of the hydroxyl groups of the pectin to aldehydes, and covalent linking of the aldehydes to a fluorescent probe (BODIPY FL hydrazide, (4,4-difluoro-5, 7-dimethyl-4-bora-3a,4a-diaza-s-indacene-3-propionylhydrazide)).

First, for the demethylesterification of pectin, plant PME was extracted from carrots (*Daucus carota* cultivar Nantes) and purified as described in the method according to Jolie et al. (2009). Purified plant PME was added to 25 mL of pectin solution (0.8% w/w high DM citrus pectin, DM ~ 95% (Sigma-Aldrich), dissolved in 0.1 M Na-phosphate buffer (pH 7.0)) and incubated for predetermined times in a water bath at 30 °C to obtain different DMs (16%, 35%, 66% and 95%). After inactivation of PME by heat treatment (4 min, 85 °C), the samples were dialyzed against demineralised water for 48 h using dialysis membranes with a MWCO of 12-14 kDa, followed by lyophilization.

Next, the samples were oxidised based on the procedure of Nordmark & Ziegler (2000). Approximately 200 mg of each lyophilised pectin sample was dissolved in 16 mL demineralised water and to the resulting pectin solution, 4 mL of 50 mM $NaIO_4$ was added. This oxidation reaction was facilitated by stirring at moderate speed for 30 min in the dark. To quench the reaction, exactly 160 µL glycerol was added and the mixture was stirred for 5 min. The oxidised sample was subsequently transferred into dialysis membranes (MWCO = 12-14 kDa) and dialyzed against demineralised water for 48 h prior to lyophilization.

In the last step, to covalently link the oxidised sample to a fluorescent label, approximately 50 mg of oxidized pectin was dissolved in 5 mL of buffer (100 mM citrate and 150 mM NaCl, pH 6) and 50 µL fluorescent label (BODIPY FL hydrazide) was added slowly (Nordmark & Ziegler,

2000). The mixture was stirred at slow speed for 4 h in the dark at room temperature to facilitate the reaction. Thereafter, 20 µL of 5 M $NaBH_3CN$ was added and the mixture was stirred for 1 h. The resulting mixture (labeled pectin sample) was consequently dialyzed (dialysis membranes with MWCO = 12-14 kDa) against 0.1 M NaCl for 24 h followed by dialysis against demineralised water for another 24 h in the dark. Prior to storage in the dark at -20 °C, the degree of labeling of the resulting pectin was measured spectrophotometrically at 340 nm (UltroSpec 2l00 Pro, GE, Uppsala, Sweden). A degree of labeling between 2 and 5 labels per 1000 GalA monomers was obtained for the pectin samples with different DMs. By controlling the pectin concentration and the molar ratio of the fluorescent label to pectin, the degree of labeling can be controlled to a great extent. In this case, approximately a 10 fold excess of the fluorescent dye was optimal, this ratio maybe varied to alter the degree of labeling. The absorbance of the resulting labeled pectin was measured spectrophotometrically at 503 nm, and using a standard curve of 0-15 µg/ml conc BODIPY FL hydrazide, the concentration of the labeled samples was established. The µmol of fluorescent label per ml of each sample was calculated and thereafter expressed as degree of labeling (which varied between 2 and 5 labels per 1000 monomers of GalA). For further use (see section 2.7), depending on the degree of labeling, different volumes were calculated to ensure that the added labeled pectins (DM 16% 35%, 66% and 95%) contained equal amounts of fluorescent label.

2.7 Reconstitution of carrot-based suspensions

HTB and LTB carrot tissue particles of a small particle fraction (80-125 µm) and a large particle fraction (>500 µm) stored on 70% ethanol were centrifuged (5 min, 22 °C and 3000 g) and washed to remove the ethanol as described by Moelants et al. (2014). The washed particles were

subsequently reconstituted. First, to evaluate the effect of the suspending medium on pectin-interactions, approximately 50 mg of particles was suspended in 500 µL of demineralised water or carrot serum. Secondly, to investigate the effect of increasing the concentration of Ca^{2+}-ions, on the one hand, 50 mg of tissue particles was weighed and 500 µL of 0.1 M $CaCl_2$ was added while on the other hand, 50 mg of particles was suspended in 500 µL of carrot serum followed by addition of 5.5 mg of $CaCl_2$. Next, the effect of pH was explored by suspending 10% w/v particles in demineralised water or serum and adjusting the pH to 2, 3.5 or 7 using either 1 M HCl or 1 M NaOH, followed by addition of 5.5 mg of $CaCl_2$. In the last step, to each of the suspensions, an appropriate amount of labeled pectin (DM 16%, 35%, 66% or 95%) was added. This step was performed in the dark to prevent bleaching of the label. The samples were thereafter vortexed at low speed and visualized under a microscope.

2.8 Visualisation of pectin-interactions in reconstituted suspensions

Pectin-interactions in the reconstituted systems were visualized using an Olympus BX-51 (Olympus, Optical Co. Ltd, Tokyo, Japan) microscope equipped with Olympus XC 50 digital camera and epifluorescence illumination (X-Cite^R Fluorescence Illumination, Series 120Q, EXFO Europe, Hants, UK). Approximately 20 µL of the suspension was placed on a glass slide, a cover slide was mounted and using objectives of 10 x and 40 x magnification, differential interference contrast light microscopy images and fluorescence microscopy images were collected. During acquisition an epifluorescence illumination was applied. A lamp supplies strong white light which is then filtered to give light of the desired wavelength. No laser was used. However, strength of the light from the lamp and the live acquisition time to make images (ms) were kept constant.

3. Results and discussion

3.1 Characterisation of pectin in carrot purées

3.1.1 Degree of methylesterification of pectin in the particle fraction and serum fraction of carrot purées

Table 1 shows the average DM values for pectin present in LTB and HTB carrot tissue particles with particle sizes of: 80-125 µm, 125-250 µm, 250-500 µm and >500 µm. It can be observed that lower DMs were obtained for pectin in LTB carrot samples compared to pectin in HTB carrot samples. In the case of LTB carrots, during incubation at 60 °C, the endogenous PME demethylesterified the pectin, resulting in low DMs. Similar results were observed by Moelants et al. (2014), in which carrot samples incubated at 60 °C for 24 h showed a lower DM of pectin compared to those blanched at 95 °C. On the other hand, high temperature blanching (of HTB samples) inactivated PME and resulted in an average high DM of pectin in the carrot tissue particles. Furthermore from the results, it can be seen that in both LTB and HTB carrot samples, the DM of pectin decreased with increasing particle size. The smaller particles (80-125 µm) exhibited higher DMs (51% and 64%, for LTB and HTB respectively) while the larger particles (>500 µm) showed lower DMs (34% and 54% for LTB and HTB samples respectively). This interesting observation is probably an indication that regions of pectin with higher and lower DM exist within carrot tissues. The regions with lower DM probably contain pectin that is strongly cross-linked through Ca^{2+}-bridges, making these regions less easily particulated into smaller particles. On the contrary, the high DM regions contain pectic polymers that are probably more loosely bound and therefore were found to be associated with smaller particles. Furthermore, the comminution of the carrots and subsequent sieving probably separated particles from different

parts of the carrot tissue. The core of the carrot, being tougher probably formed the larger particles while the softer parts of the carrot were easier to comminute into smaller particles. Finally from Table 1, it can also be observed that serum pectin from LTB carrot samples exhibited a lower DM (34%) compared to the DM of pectin of HTB serum samples (76%). This observation is in line with the generally lower DMs for pectin in LTB carrot tissue particles compared to the higher DMs for pectin in HTB carrot tissue particles. In addition, the degree of blockiness (DB) of serum pectin predicted as described by Ngouémazong et. (2011) revealed that LTB serum pectin had a higher DB (84.6%) compared to the DB of HTB serum pectin (64.1%).

3.1.2 Galacturonic acid and neutral sugar content of carrot serum pectin

As can be seen from Figure 1, GalA contents of 137 and 326 mg/g of sample were obtained for LTB and HTB carrot serum samples, respectively. The samples showed relatively low amounts of the pectin-related sugars fucose, rhamnose (Rha) and xylose. On the other hand, appreciable to high amounts of the pectin-related neutral sugars arabinose (Ara) and galactose (Gal) were observed, with LTB carrot serum samples exhibiting higher amounts compared to HTB carrot serum samples. Considering the ratio of the molar amounts of GalA to the sum of molar amounts of Fuc, Rha, Ara, Gal and Xyl, which is a measure for the linearity of pectin, it was noticed that pectin of HTB carrot serum exhibited higher linearity (GalA/(Fuc + Rha + Ara + Gal + Xyl) = 2.2) compared to pectin of LTB carrot serum samples (GalA/(Fuc + Rha + Ara + Gal + Xyl) = 0.5). As HTB carrot serum pectin was more linear, it was therefore less branched compared to LTB carrot serum pectin. Owing to the fact that pectin of LTB carrot samples generally exhibited a lower DM, this pectin was probably more strongly bound in the carrot cell walls through Ca^{2+} cross-links. Considering that these Ca^{2+} cross-linked pectin polymers are generally more linear, the linear GalA rich pectin in LTB carrot cell walls was thus more strongly bound. Hence, only

357 the less linear pectin (more branched pectin) leached to the serum as it was less resistant to
358 leaching than the more linear Ca^{2+} cross-linked pectin. On the other hand, pectin of HTB carrots
359 was of higher DM, therefore, most of this pectin was less strongly bound in the cell walls,
360 allowing more of the linear pectin to leach out into the serum.

361 **3.1.3 Molar mass distribution of carrot serum pectin**

362 Molar mass and concentration profiles obtained for serum pectins from LTB and HTB carrot
363 purées are presented in Figure 2. In general, from the molar mass profiles (represented by dotted
364 lines), as elution time increases, molar mass of the eluted components decreases. This trend is as
365 expected based on the working principle of high-performance size exclusion chromatography,
366 where based on hydrodynamic volume, smaller molecules travel a longer distance and elute later
367 than larger molecules. As can be seen from the concentration profiles (represented by full lines),
368 pectin from both LTB and HTB carrot serum exhibited two elution peaks. Serum pectin from
369 LTB carrot samples showed lower concentrations for the pectin with larger mean molar mass
370 (2.06×10^7 Da) and higher concentrations for pectin with smaller average molar mass (1.15×10^6
371 Da). For the serum of the HTB carrot samples, the larger pectic polymers (6.01×10^6 Da)
372 exhibited a higher concentration while the smaller molecules (1.01×10^6 Da) showed a lower
373 contribution. For the LTB carrot serum samples, considering that the DM of the pectin was
374 generally lower, more pectin was probably cross-linked through Ca^{2+}-bridges. Hence, pectin with
375 higher molar mass was probably well retained in the tissue while the lower molar mass pectins
376 were nevertheless more easily leached into the serum. The low concentrations of higher molar
377 mass pectins obtained for LTB carrot serum samples could also be attributed to limited
378 filterability. It might have been that some of the pectin (Ca^{2+} cross-linked, highly branched
379 pectin) that leached in to the serum of LTB carrots was larger than the filter used (0.45 µm).

Therefore, only the pectic polymers with smaller molar mass were filterable, resulting in lower concentrations of the larger pectic polymers. On the other hand, for the HTB carrot samples, due to higher DM of pectin, there was less Ca^{2+} mediated pectin-pectin interaction. Hence, more of the high molar mass pectins could leach to the serum more easily. In general, it can be concluded that, depending on the treatment applied, during subsequent mechanical disintegration, pectins with different characteristics leached into the serum of carrot suspensions.

3.2 Visualisation of Ca^{2+} mediated pectin-pectin interactions in reconstituted carrot-based suspensions

3.2.1 Identification of particle types in LTB and HTB reconstituted carrot-based suspensions

3.2.1.1 Light microscopy

Figure 3 presents the light microscopy images of smaller particles (80-125 µm) and larger clusters (>500 µm) of LTB and HTB carrot samples. It can be observed that carrot tissue particles are made up of parenchyma cells with an average diameter of ~70 µm (Day, Xu, Oiseth, Hemar, & Lundin, 2010). In addition, it can be observed that by mechanical disruption of carrot tissues, for LTB carrot, cell breakage occurred as indicated by the rough edges of broken cells while in the case of HTB carrot samples, different tissue particles were obtained mainly through cell separation. During incubation of LTB carrot samples, by the action of endogenous PME, pectin of low DM was created (see section 3.1.1). This pectin was probably strongly cross-linked through Ca^{2+}-bridges, resulting in cell breakage rather than cell separation during mechanical disintegration. On the other hand, in the case of HTB carrots, due to absence of PME activity, the

high DM of pectin was maintained. As high DM pectin is likely to be more loosely bound, cell separation was occurred during mechanical disruption.

3.2.1.2 Immunolabeling of pectin at the surface of carrot tissue particles

The results of immunolabeling of tissue particle (>500 um) surfaces of LTB and HTB carrots are represented in Figure 4. Only results for immunolabeling of larger cell clusters are shown as similar results were obtained for both cases of larger cell clusters and smaller cell clusters. Using JIM7 which is a general anti-pectin antibody but with stronger binding to high methylesterified pectin, particles from HTB carrot samples showed more fluorescence than particles from LTB carrot samples which is a reflection of the higher DM of pectin in HTB treated samples. PAM1 was used, for detection of low methylesterified pectin regions using PAM1. Particles of the LTB carrot samples showed more PAM1 labeling compared to those of HTB carrot samples. This observation can be related to the action of endogenous PME during incubation of the LTB samples, resulting in low DM pectin. Similarly, Ca^{2+} cross-linked pectin regions were observed for both LTB and HTB carrot samples using the 2F4 antibody and presence of these regions was more pronounced in the LTB particles which showed the lowest DM (34%). This can be attributed to the blockwise action of PME during incubation of LTB carrot samples, producing consecutive blocks of non-methylesterified GalA residues that have the potential to cross-link through Ca^{2+}-ions.

3.2.2 Calcium mediated pectin-pectin interactions in LTB and HTB carrot tissue particles reconstituted in demineralised water or serum, with or without added Ca^{2+}-ions

Ca^{2+} mediated pectin-pectin interactions were visualized for small and large LTB and HTB carrot tissue particles reconstituted in either demineralised water or carrot serum. In both cases,

423 the effect of increasing the amount of Ca^{2+}-ions was also studied as shown in Figures 5. Figure
424 5A and B represent interactions of pectin at the surface of tissue clusters of LTB carrot samples
425 while Figure 5C shows results of HTB carrot samples.

426 **3.2.2.1 LTB carrot-based suspensions**

427 For LTB carrot samples, Figure 5A shows results for suspensions reconstituted with smaller
428 particles (80-125 µm) while Figure 5B represents results for suspensions reconstituted with
429 larger clusters (>500 µm). For the 80-125 µm clusters (containing pectin with average DM of
430 51%), reconstituted in demineralised water (Figure 5A), in the presence of labeled pectin with a
431 DM of 16%, less intense Ca^{2+} mediated pectin-pectin interactions indicated by low intensity
432 fluorescence were observed at the surface of the LTB carrot particles while no fluorescence of
433 labeled pectin was visible in the background. For LTB carrot tissue particles with larger sizes
434 (>500 µm) shown in Figure 5B, similar results were observed. In this case, the fluorescence was
435 slightly more intense, as the DM of pectin in the tissue particles was lower (DM 34%). As the
436 DM of the labeled pectin was increased, no interaction was observed between the labeled pectin
437 and the pectin at the surface of the smaller tissue particles while in the case of larger particles
438 decreasing fluorescence of the particle surfaces was observed (shown by red arrows). In fact,
439 when labeled pectins of DMs 66 and 95% were added, the smaller particle surfaces did not
440 exhibit any fluorescence while more intense fluorescence was visible in the background. From
441 these results, it can therefore be noted that despite the high DM (51%) of pectin at the surface of
442 the smaller particles (80-125 µm) and no extra Ca^{2+}-ions added, labeled pectin with the lowest
443 DM (16%) was able to initiate weak cross-linking. On the other hand, the lower DM of pectin in
444 the larger particles (>500 µm), promoted slightly better cross-linking than in the case of smaller
445 clusters (shown by blue arrows). By increasing the DM of labeled pectin, the cross-linking was

446 no longer initiated in the smaller particles, while in larger clusters, the cross-linking decreased
447 with increasing DM of labeled pectin.

448 When the concentration of Ca^{2+}-ions was increased by addition of 0.1 M $CaCl_2$, more intense
449 Ca^{2+} mediated pectin-pectin interactions were visible, with the highest interactions visible in
450 presence of labeled pectin with the lowest DM (16%). In presence of labeled pectin of DMs
451 35%, 66% and 95%, less intense interactions were observed compared to the case where labeled
452 pectin with a DM of 16% was used. In the latter cases, the high fluorescence intensity of the
453 background indicated that there was more labeled pectin in the background than at the particle
454 surfaces. From the pictures of particles of LTB carrot samples reconstituted in water with added
455 Ca^{2+}, it can generally be observed that fluorescence of the surfaces of the larger clusters was
456 more intense than that of the smaller clusters (as shown by the black arrows). This can be
457 explained by the fact that the larger particles exhibited a lower DM (34%) of pectin and as
458 described by Thibault & Ralet (2003), low methylesterified pectins with a blockwise distribution
459 of free carboxyl groups by the action of carrot PME are very sensitive to calcium. Therefore,
460 they were able to form more intense Ca^{2+} mediated pectin-pectin interactions with labeled pectin,
461 especially with labeled pectin of DM 16%.

462 When LTB carrot tissue particles were reconstituted in LTB carrot serum, less intense
463 interactions were observed between the particles and labeled pectin of DMs 16% and 35% for
464 the smaller clusters (indicated by the grey arrow). With labeled pectin of high DM (DM 66% and
465 95%), no fluorescence was observed at the particle surfaces. For the larger clusters, similar
466 results were observed. In both cases (larger and smaller clusters), interaction between labeled
467 pectin and pectin at the surface of particles was observed despite presence of soluble pectin in
468 the serum (DM 34%) which was expected to be a competition factor for interaction with labeled

pectin. This observation can be attributed to the fact that LTB serum pectin is strongly branched and exhibits generally a low molar mass, thus generating little competition for labeled pectin, despite its low DM and high degree of blockiness (84.6%). Although the fluorescence of the surfaces of particles was observed (more intense for larger particles than in the case of smaller particles reconstituted in serum), it was less intense than that for particles reconstituted in water.

As the Ca^{2+} concentration was increased for the suspensions reconstituted in serum, Ca^{2+} mediated pectin-pectin interactions intensified for all cases, with the most intense interactions observed in presence of labeled pectin of DM 16% (shown by the discontinuous grey arrow). In presence of labeled pectin of the other DMs (35%, 66% and 95%), fluorescence of the background is still an indication that less of the labeled pectin is interacting with pectin at the surface of tissue particles.

3.2.2.2 HTB carrot-based suspensions

In the case of HTB treated carrot samples, the results obtained for suspensions reconstituted with smaller carrot tissue particles (80-125 µm) are presented in Figure 5C. Specifically, smaller particles, particularly those of 80-125 µm exhibited a DM of 64% while larger particles of diameter >500 µm (results not shown) exhibited a slightly lower DM (54%). For the 80-125 µm particles reconstituted in demineralised water (Figure 5C), very low interaction between labeled pectin (DM 16%) and pectin at the HTB carrot particle surfaces was observed (shown by a red arrow). In the case of larger clusters (results not shown), better interactions between labeled pectin and pectin at the surface of the particles was observed. Shifts in gray value as illustrated in supplementary Figure 1 complimented this observation. Even at this lowest DM of labeled pectin (DM 16%), the fluorescence was very weak for the smaller particles, which can be attributed to

the DM of pectin of the carrot cell clusters (64%) not being low enough to facilitate Ca^{2+} mediated pectin-pectin interaction. In presence of labeled pectin of DMs 35%, 66% and 95%, no interactions were observed for the smaller clusters while less intense interactions were observed for the larger clusters (shown by red arrows).

As the amount of Ca^{2+}-ions was increased, more fluorescence of the tissue particles was observed (shown by the black arrow), indicating increased Ca^{2+} mediated pectin-pectin interactions especially in presence of labeled pectin of the lowest DM (16%) (see further, supplementary Figure 1). By increasing the DM of labeled pectin to 35%, 66% and 95%, less intense Ca^{2+} mediated pectin-pectin interactions were possible between pectin at the surfaces of particles and labeled pectin. In general, the interactions between labeled pectin and pectin in smaller particles were weaker than those between labeled pectin and pectin in larger clusters. As in the case of LTB carrot tissue particles, this observation can generally be attributed to the lower DM (54%) of pectin present in larger clusters compared to the higher DM of pectin present in smaller clusters.

When HTB carrot tissue particles were reconstituted in HTB carrot serum, very low interactions with labeled pectin were observed without added Ca^{2+} for both smaller clusters (Figure 5C, indicated by the grey arrow) and larger clusters (results not shown). These interactions were less intense than those observed for particles reconstituted in water. This observation was further illustrated by a lower gray value in presence of serum (supplementary Figure 2). The weaker fluorescence, thus low interaction between labeled pectin and pectin at the surfaces of HTB particles in presence of serum is probably due to the competition for labeled pectin created by presence of linear pectin in HTB serum.

By increasing the Ca^{2+} concentration in these suspensions (of HTB particles in HTB carrot serum), interaction between labeled pectin and pectin at the surface of the tissue particles was only slightly improved (indicated by a grey discontinuous arrow). This could be attributed to the soluble pectin present in the serum acting as a competition factor despite its high DM (76%) and lower degree of blockiness (64.1%). As mentioned earlier, pectin present in the HTB serum was more linear compared to LTB serum pectin, therefore it was able to compete with pectin at the surface of the particles for labeled pectin, preventing pronounced Ca^{2+} mediated pectin-pectin interaction at the particle surfaces.

In general, it can be concluded that pectin in LTB carrot tissue particles exhibited more intense interactions with labeled pectin compared to pectin in HTB carrot tissue particles. Furthermore, it can be concluded that Ca^{2+} mediated pectin-pectin interactions are dependent on both the DM of the labeled pectin and the DM of pectin at the surface of the tissue particles, as well as the concentration of Ca^{2+}-ions. The influence of the serum phase on pectin-Ca^{2+} interactions depends on the characteristics of pectin present in the serum. Finally, the strongest pectin-Ca^{2+} interactions were obtained at the lowest DM studied.

3.5.3 Ca^{2+} mediated pectin-pectin interactions at different pH conditions

The effect of pH on pectin-interactions was investigated at three pH conditions (pH 2, 3.5 and 7). The pH conditions were selected based on the fact that the pKa value of pectin varies between 3.38 and 4.10 (Moore, 1985; Manrique & Lajolo, 2002; Sriamornsak, 2003). In this context, a pH close to the pKa value (pH 3.5) was selected. At this pH value, 50% of the carboxyl groups of pectin are ionized (Sriamornsak, 2003). Additionally, two other pH conditions were explored. A pH condition at which there is a predominance of non-dissociated acid groups (pH 2, i.e.,

535 below pKa value of pectin) and one at which the net charge is negative (pH 7, i.e., above pKa
536 value of pectin). In Figure 5D, the results obtained for LTB and HTB carrot tissue particles
537 reconstituted in demineralised water, in presence of added Ca^{2+} and labeled pectin of the lowest
538 DM (DM 16%) are presented. As can be seen from the images, at pH 2, the fluorescence at the
539 surface of the tissue particles is less/weaker compared to the other pH conditions (pH 3.5 and 7).
540 Furthermore, gray values obtained at this pH were lower than those at pH 3,5 and 7
541 (supplementary Figure 3). In addition, a lot of fluorescence is seen in the background, which also
542 supports that there is less preference for interaction between labeled pectin and pectin at the
543 surface of tissue particles. At this pH only a few of the carboxyl groups are negatively charged,
544 therefore less Ca^{2+}-mediated electrostatic interactions are possible. As the pH increases to pH
545 3.5, more fluorescence is observed with less of the labeled pectin in the background. This is
546 attributed to the fact that at this pH, 50% of the carboxyl groups are ionized (negatively charged)
547 thus more interaction of pectin at the surface of the particles with labeled pectin in presence of
548 Ca^{2+} is present, leaving less labeled pectin in the background. Finally at pH 7, almost complete
549 ionization of all carboxylate groups has been attained. Hence, more charged pectin is present to
550 cross-link through Ca^{2+} to labeled pectin. This is evidenced by the increased fluorescence of the
551 tissue particle surfaces and a background depleted of labeled pectin. This trend was also
552 observed in presence of labeled pectins of DMs 35%, 66% and 95% (results not shown) but in
553 these cases, the interactions became less intense with increasing DM of the labeled pectin. In
554 both cases (LTB and HTB carrot tissues), larger tissue particles (>500 µm) exhibited better Ca^{2+}
555 mediated pectin-pectin interaction owing to the lower DMs compared to smaller particles (80-
556 125 µm). Finally, it can generally be concluded that in presence of Ca^{2+}-ions, Ca^{2+} mediated
557 pectin-pectin interactions increased with increasing pH.

5. Conclusion

Enhanced insight into Ca^{2+} mediated pectin-pectin interactions occurring in selectively processed particulated products can be obtained by exploring the interaction between fluorescently labeled pectin and pectin at the surface of the tissue particles or in the liquid phase. Using this method, Ca^{2+} mediated pectin-pectin interactions can be visualised *in situ* (without prior isolation of pectin from plant tissues, eliminating the possibility of changes in pectin structure). The fluorescence of labeled pectin under epifluorescence illumination can be used to evaluate the occurrence of pectin-interactions, and the extent to which specific factors affect these interactions. In particular, this research provides visual evidence of the dependence of pectin-interactions on the DM of pectin, the concentration of Ca^{2+}-ions and pH.

Acknowledgements

The authors acknowledge the financial support of KU Leuven Research long term structural funding - Methusalem funding by the Flemish Government. C. Kyomugasho is a Ph.D. Fellow funded by the interfaculty Council for Development Co-operation (IRO). S. Christiaens is a Postdoctoral Researcher funded by Research Foundation Flanders (FWO).

Reference List

Ahmed, A. & Labavitch, J. M. (1977). A simplified method for accurate determination of cell wall uronide content. *Journal of Food Biochemistry*, 361-365.

Blumenkrantz, N. & Asboe-Hansen, G. (1973). New method for quantitative determination of Uronid acids. *Analytical Biochemistry*, 484-489.

580 Brummell, D. A. (2006). Cell wall disassembly in ripening fruit. *Functional Plant Biology, 33,*
581 103-119.

582 Caffall, K. H. & Mohnen, D. (2009). The structure, function, and biosynthesis of plant cell wall
583 pectic polysaccharides. *Carbohydrate Research, 344,* 1879-1900.

584 Christiaens, S., Mbong, V. B., Van Buggenhout, S., David, C. C., Hofkens, J., Van Loey, A. M.
585 et al. (2012). Influence of processing on the pectin structure-function relationship in
586 broccoli puree. *Innovative Food Science & Emerging Technologies, 15,* 57-65.

587 Christiaens, S., Van Buggenhout, S., Vandevenne, E., Jolie, R., Van Loey, A. M., & Hendrickx,
588 M. E. (2011). Towards a better understanding of the pectin structure-function relationship
589 in broccoli during processing: Part II - Analyses with anti-pectin antibodies. *Food*
590 *Research International, 44,* 2896-2906.

591 Day, L., Xu, M., Oiseth, S. K., Hemar, Y., & Lundin, L. (2010). Control of Morphological and
592 Rheological Properties of Carrot Cell Wall Particle Dispersions through Processing. *Food*
593 *Bioprocess Technol, 3,* 928-934.

594 Fraeye, I., Doungla, E., Duvetter, T., Moldenaers, P., Van Loey, A., & Hendrickx, M. (2009).
595 Influence of intrinsic and extrinsic factors on rheology of pectin-calcium gels. *Food*
596 *Hydrocolloids, 23,* 2069-2077.

597 Haghighi, M. & Rezaei, K. (2012). Review Article: General Analytical Schemes for the
598 Characterisation of Pectin-Based Edible Gelled Systems. *The Scientific World Journal*.

599 Houben, K., Jolie, R. P., Fraeye, I., Van Loey, A. M., & Hendrickx, M. E. (2011). Comparative
600 study of the cell wall composition of broccoli, carrot, and tomato: Structural
601 characterization of the extractable pectins and hemicelluloses. *Carbohydrate Research, 346,* 1105-1111.

603 Ishii, T., Ichita, J., Matsue, H., Ono, H., & Maeda, I. (2002). Fluorescent labeling of pectic
604 oligosaccharides with 2-aminobenzamide and enzyme assay for pectin. *Carbohydrate*
605 *Research, 337,* 1023-1032.

606 Jolie, R. P., Duvetter, T., Houben, K., Clynen, E., Sila, D. N., Van Loey, A. M. et al. (2009).
607 Carrot pectin methylesterase and its inhibitor from kiwi fruit: Study of activity, stability
608 and inhibition. *Innovative Food Science & Emerging Technologies, 10,* 601-609.

609 Kim, Y. & Wicker, L. (2011). Charge domain of modified pectins influence interaction with
610 acidified caseins. *Food Hydrocolloids, 25,* 419-425.

611 Kyomugasho, C., Christiaens, S., Shpigelman, A., Van Loey, A. M., & Hendrickx, M. E. (2015).
612 FT-IR spectroscopy, a reliable method for routine analysis of the degree of
613 methylesterification of pectin in different fruit- and vegetable-based matrices. *Food*
614 *Chemistry, 176,* 82-90.

615 Lofgren, C. & Hermansson, A. M. (2007). Synergistic rheological behaviour of mixed HM/LM
616 pectin gels. *Food Hydrocolloids, 21,* 480-486.

617 Lopez-Sanchez, P., Nijsse, J., Blonk, H. C. G., Bialek, L., Schumm, S., & Langton, M. (2011).
618 Effect of mechanical and thermal treatments on the microstructure and rheological

properties of carrot, broccoli and tomato dispersions. *Journal of the Science of Food and Agriculture, 91,* 207-217.

Manrique, G. D. & Lajolo, F. M. (2002). FT-IR spectroscopy as a tool for measuring degree of methyl esterification in pectins isolated from ripening papaya fruit. *Postharvest Biology and Technology, 25,* 99-107.

McFeeters, R. F. (1985). Changes in Pectin and Celullose during Processing. In T. Richardson & J. W. Finley (Eds.), *Chemical changes in Food during Processing* (pp. 347-372).

Mcfeeters, R. F. & Armstrong, S. A. (1984). Measurement of pectin methylation in plant-cell walls. *Analytical Biochemistry, 139,* 212-217.

Moelants, K. R. N., Cardinaels, R., De Greef, K., Daels, E., Van Buggenhout, S., Van Loey, A. M. et al. (2014). Effect of calcium ions and pH on the structure and rheology of carrot-derived suspensions. *Food Hydrocolloids, 36,* 382-391.

Moore, D. S. (1985). Amino acid and peptide net charges: A simple calculational procedure. *Biochemical Education, 13,* 10-11.

Ngouémazong, D. E., Tengweh, F. F., Duvetter, T., Fraeye, I., Van Loey, A., Moldenaers, P. et al. (2011). Quantifying structural characteristics of partially de-esterified pectins. *Food Hydrocolloids, 25,* 434-443.

Nordmark, T. S. & Ziegler, G. R. (2000). Quantitative assessment of phase composition and morphology of two-phase gelatin–pectin gels using fluorescence microscopy. *Food Hydrocolloids, 14,* 579-590.

Ridley, B. L., O'Neill, M. A., & Mohnen, D. (2001). Pectins: structure, biosynthesis, and oligogalacturonide-related signaling. *Phytochemistry, 57,* 929-967.

Sanchez, P. L. (2011). *Microstructure and Rheological Properties of Plant Particle Suspensions Prepared Using Different Physical Treatments*. Chalmers University of Technology.

Shpigelman, A., Kyomugasho, C., Christiaens, S., Van Loey, A. M., & Hendrickx, M. E. (2014). Thermal and high pressure high temperature processes result in distinctly different pectin non-enzymatic conversions. *Food Hydrocolloids, 39,* 251-263.

Sila, D., Van Buggenhout, S., Duvetter, T., Fraeye, I., De Roeck, A., Van Loey, A. et al. (2009). Pectins in Processed Fruit and Vegetables: Part II - Structure-Function Relationships. *Comprehensive Reviews in Food Science and Food Safety, 8,* 86-104.

Sriamornsak, P. (2003). Chemistry of pectin and its pharmaceutical uses: A review. *Silpakorn University International Journal, 3,* 206-228.

Strom, A., Lundin, L., Morris, E. R., & Williams, M. A. K. (2012). Relation between Rheological Properties of Pectin Gels and Pectin Structure. In *Annual Transactions of the Nordic rheology society*.

Strom, A., Ribelles, P., Lundin, L., Norton, I., Morris, E. R., & Williams, M. A. K. (2007). Influence of Pectin Fine Structure on the Mechanical Properties of Calcium–Pectin and Acid–Pectin Gels. *Biomacromolecules, 8,* 2668-2674.

657 Szymanska-Chargot, M. & Zdunek, A. (2013). Use of FT-IR Spectra and PCA to the Bulk
658 Characterization of Cell Wall Residues of Fruits and Vegetables Along a Fraction
659 Process. *Food Biophysics, 8,* 29-42.

660 Thakur, B. R., Singh, R. K., & Handa, A. K. (1997). Chemistry and uses of pectin - A review.
661 *Critical Reviews in Food Science and Nutrition, 37,* 47-73.

662 Thibault, J.-F. & Ralet, M.-C. (2003). Physico-chemical properties of pectin in the cell walls and
663 after extraction. In *Advances in pectin and pectinase research* (pp. 91-105). Kluwer
664 academic publishers.

665 Tromp, R. H., de Kruif, C. G., van Eijk, M., & Rolin, C. (2004). On the mechanism of
666 stabilisation of acidified milk drinks by pectin. *Food Hydrocolloids, 18,* 565-572.

667 Voragen, A. G. J., Coenen, G. J., Verhoef, R. P., & Schols, H. A. (2009). Pectin, a versatile
668 polysaccharide present in plant cell walls. *Structural Chemistry, 20,* 263-275.

669 Yapo, B. M., Lerouge, P., Thibault, J. F., & Ralet, M. C. (2007). Pectins from citrus peel cell
670 walls contain homogalacturonans homogenous with respect to molar mass,
671 rhamnogalacturonan I and rhamnogalacturonan II. *Carbohydrate Polymers, 69,* 426-435.

672

673 **Figure captions**

674 **Figure 1.** Absolute GalA and neutral sugar content of LTB serum pectin (▬) and HTB serum
675 pectin (▭) with the associated standard deviations.

Figure 2. Molar mass and concentration profiles of LTB serum pectin and HTB serum pectin. Dotted lines represent the molar mass profiles (•• LTB and •• HTB) and full lines represent concentration profiles (▬LTB and ▬HTB).

Figure 3. Representative light microscopy images of particles from LTB and HTB processed carrot tissues. Particles of 80-125 µm and >500 µm are shown. Scale bars = 100 µm.

Figure 4. Representative images of immunofluorescence labeling of tissue particle surfaces of LTB and HTB carrots with JIM7, PAM1 and 2F4. Results of particles >500 µm are shown. Scale bars = 500 µm.

Figure 5. Representative images of Ca^{2+} mediated pectin-pectin interactions between fluorescently labeled pectin (DM 16%, 35%, 66% and 95%) and pectin at the surfaces of tissue particles of processed carrots. The particles were reconstituted in either demineralised water (+ Ca^{2+}) or serum (+ Ca^{2+}). (A) represents particles of 80-125 µm (DM 51%) while (B) shows images of particles sizes >500 µm (DM 34%) of LTB carrots and (C) represents particles of 80-125 µm (DM 64%) of HTB carrots. Scale bars = 500 µm. (D) represents images of Ca^{2+} mediated pectin-pectin interactions between fluorescently labeled pectin (DM 16%) and pectin at surfaces of tissue particles of 80-125 µm (with DM of 51% and 64% for LTB and HTB carrot samples, respectively) as a function of pH. Scale bars = 100 µm.

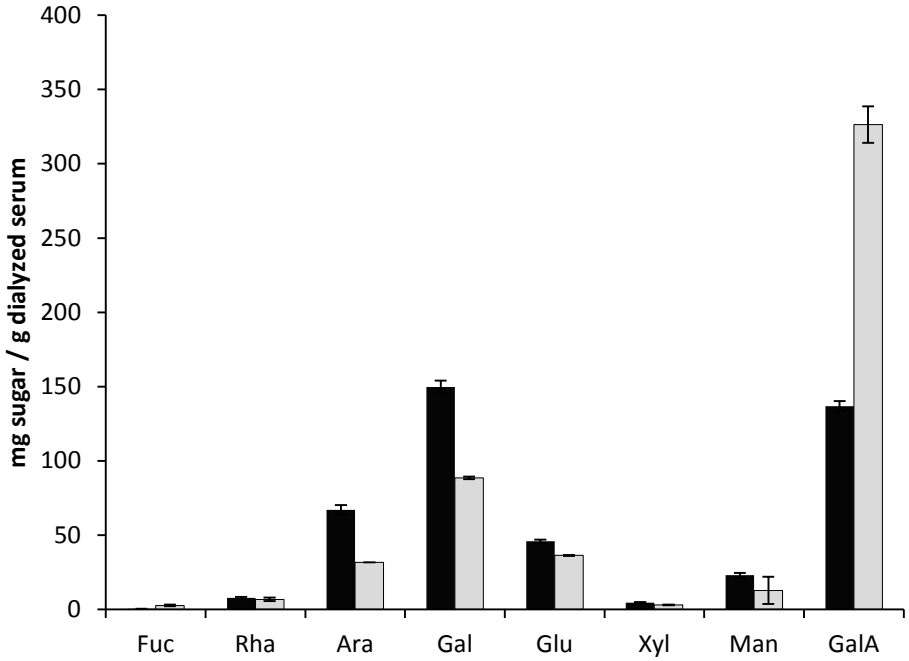

Figure 1

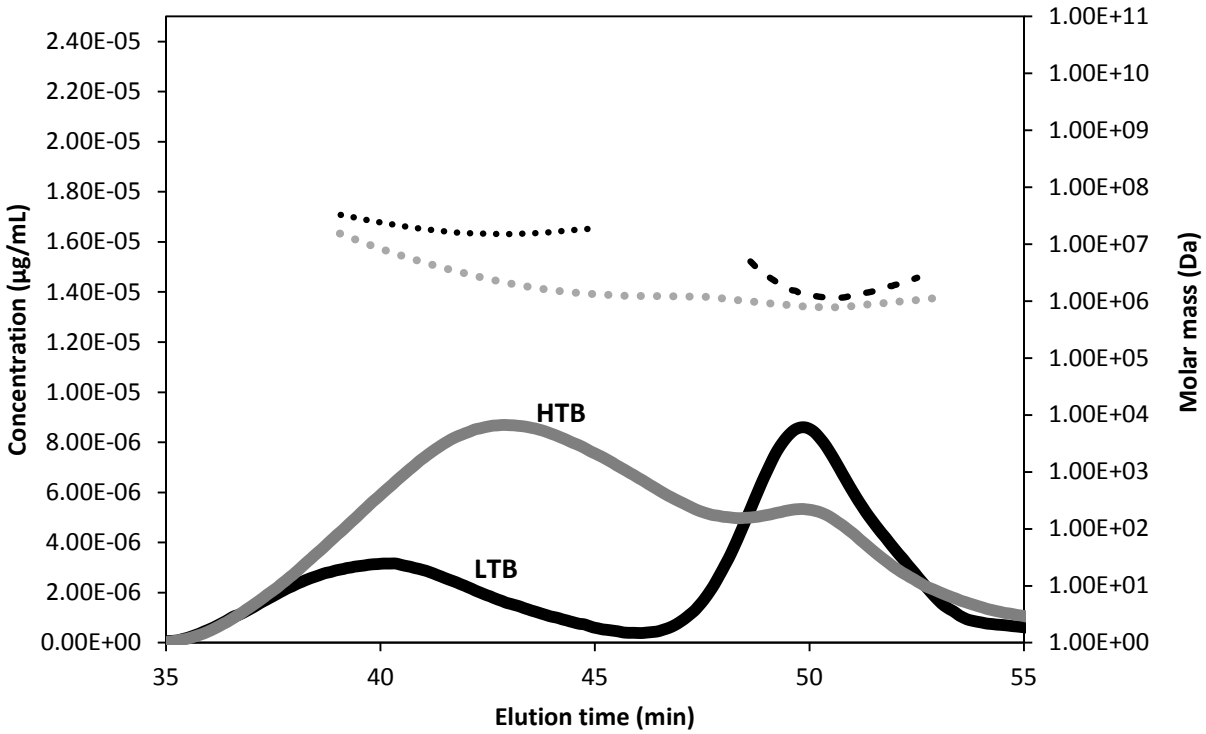

Figure 2

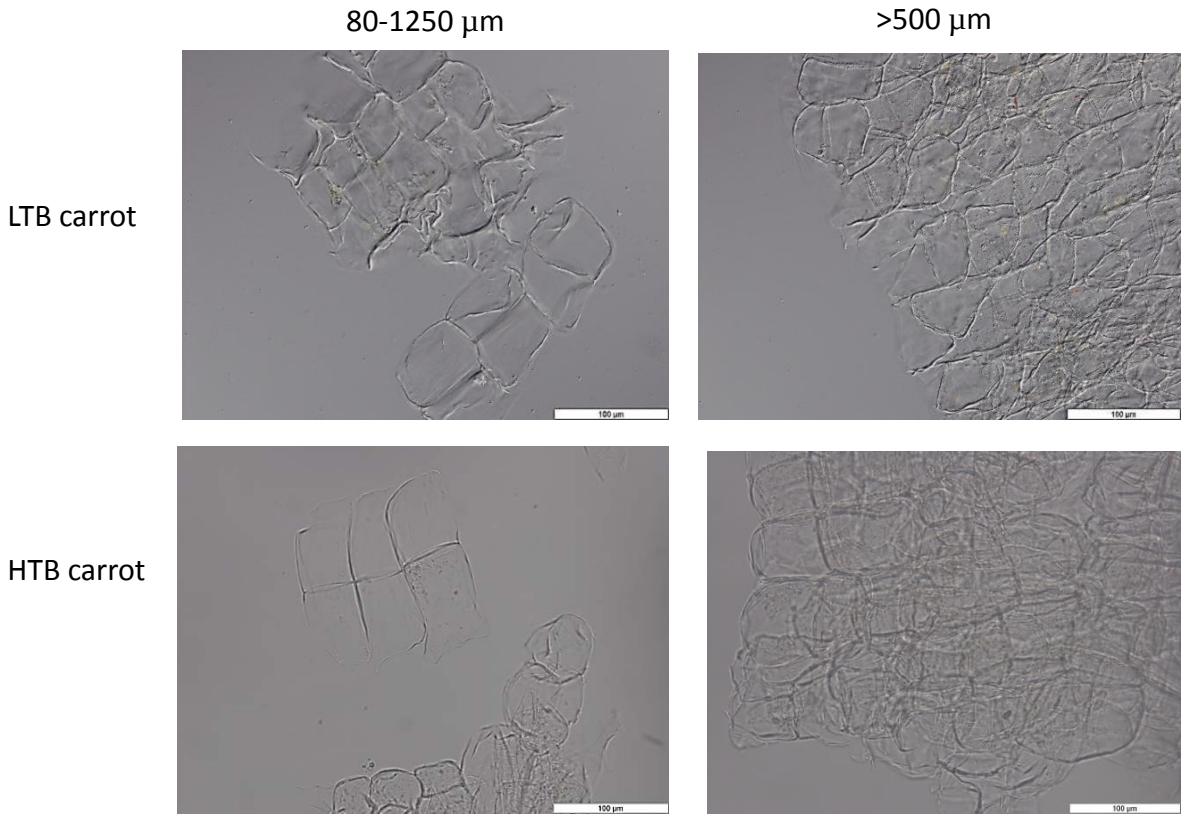

Figure 3

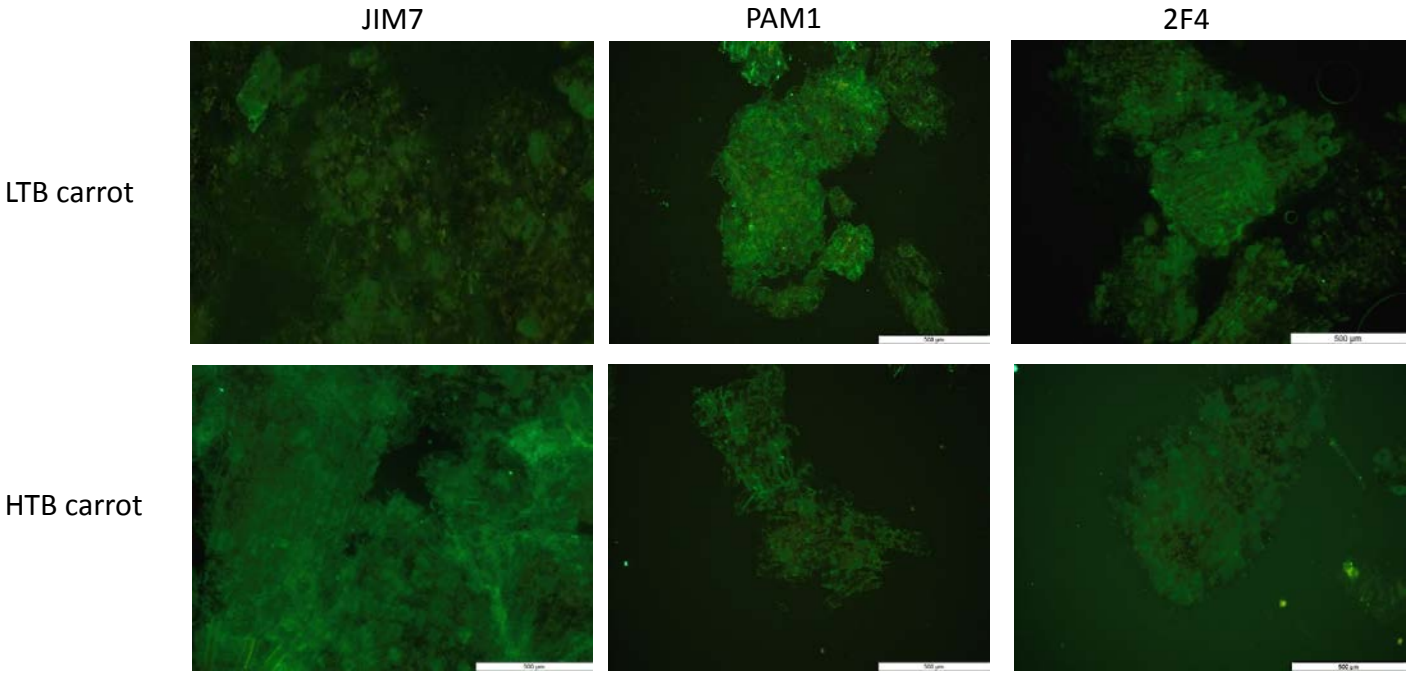

Figure 4

$LTB_{carrot\ tissue\ particles}$ =80-125 µm

$DM_{tissue\ particles}$ = 51%

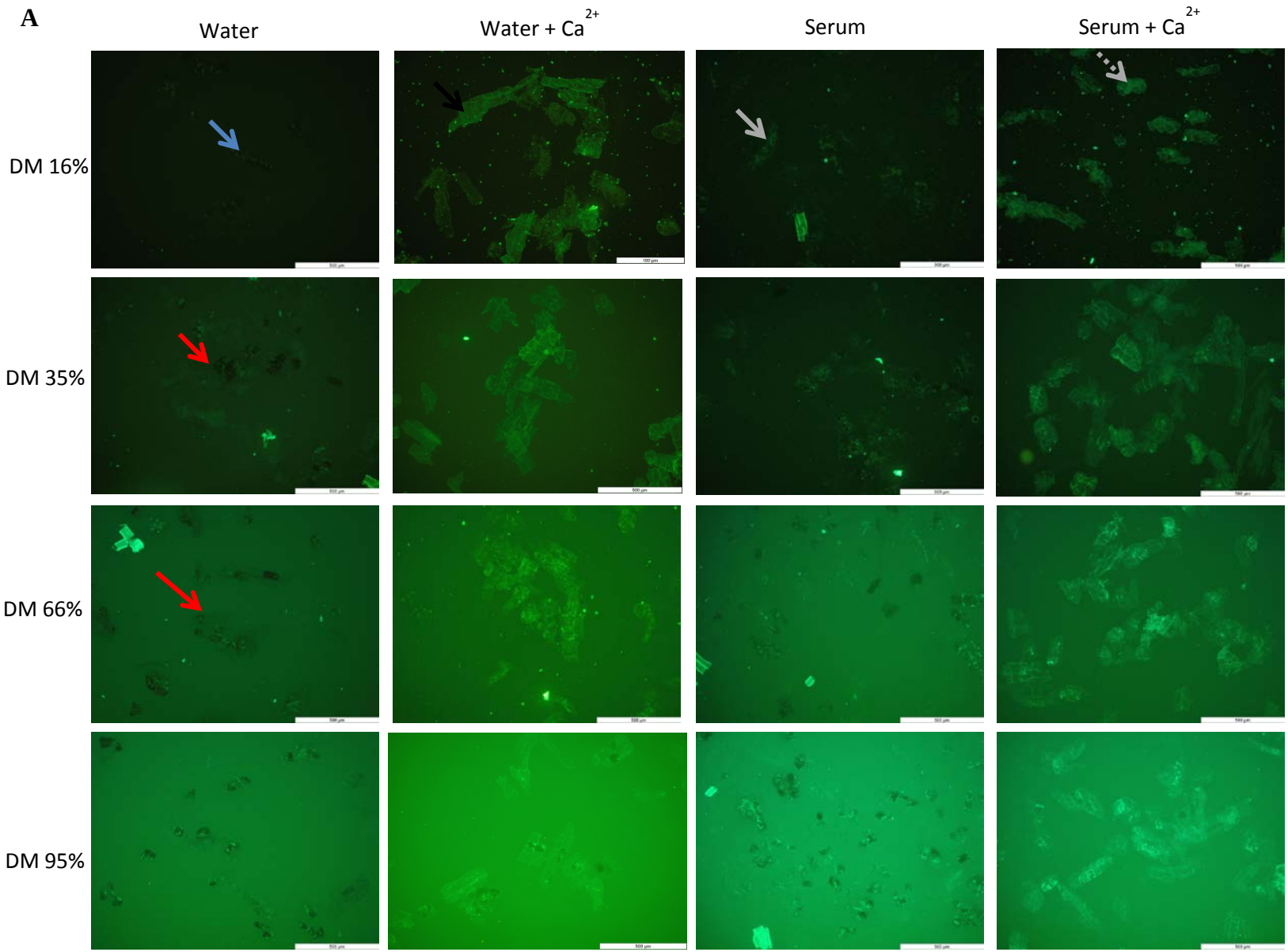

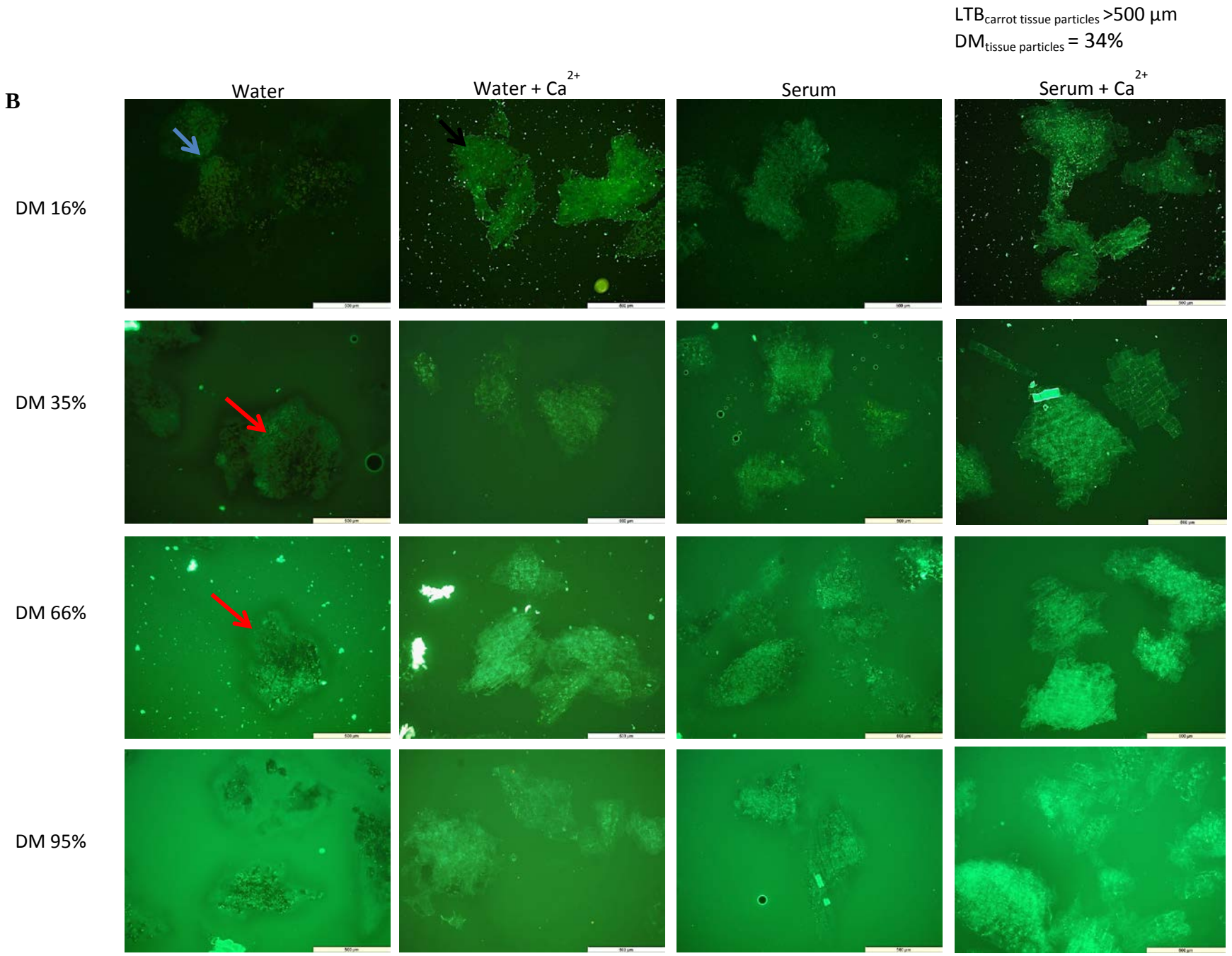
LTB carrot tissue particles >500 µm
DM tissue particles = 34%
B
Water
Water + Ca2+
Serum
Serum + Ca2+
DM 16%
DM 35%
DM 66%
DM 95%

$HTB_{carrot\ tissue\ particles}$ 80-125 µm
$DM_{tissue\ particles}$ = 64%

C

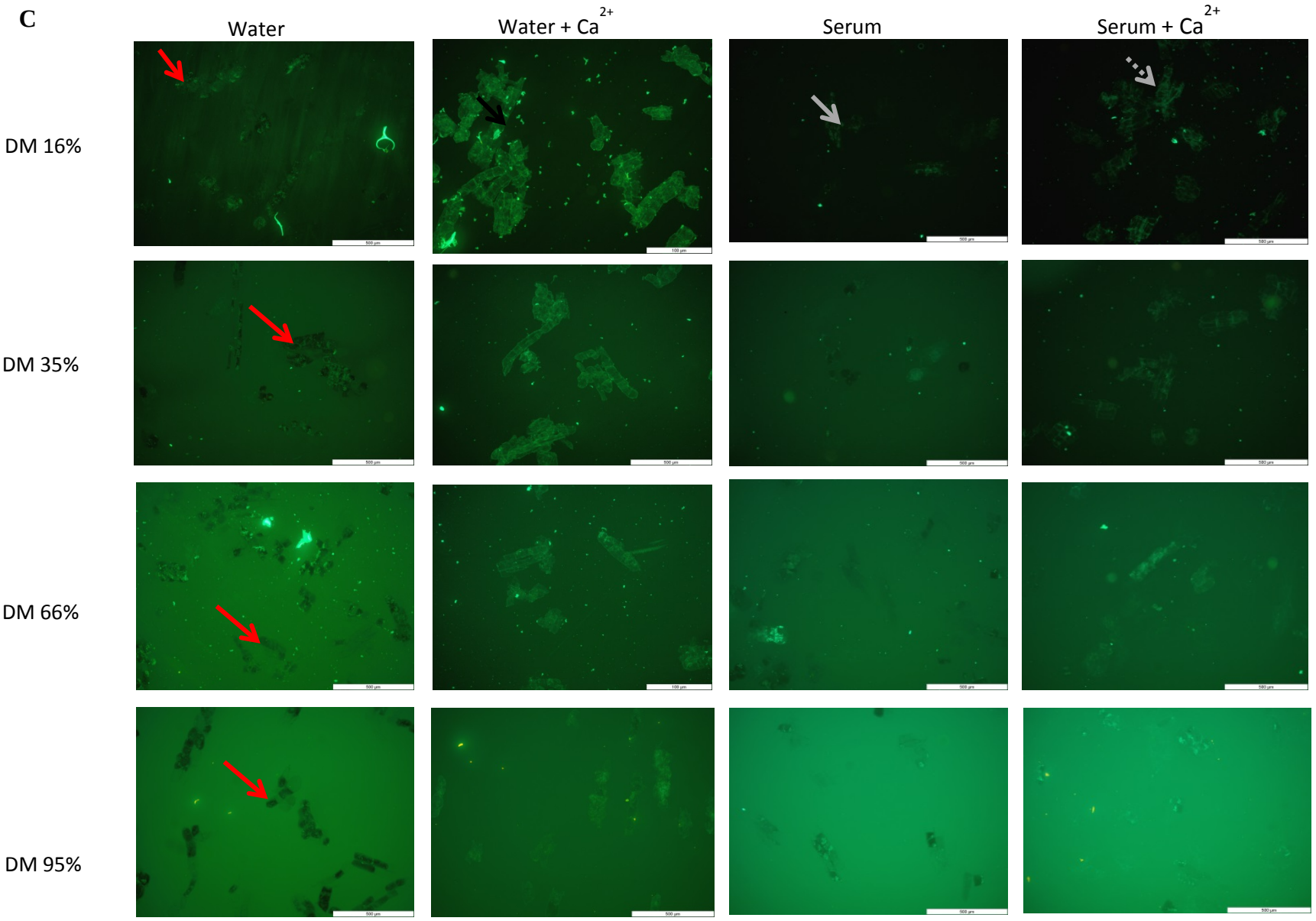

D

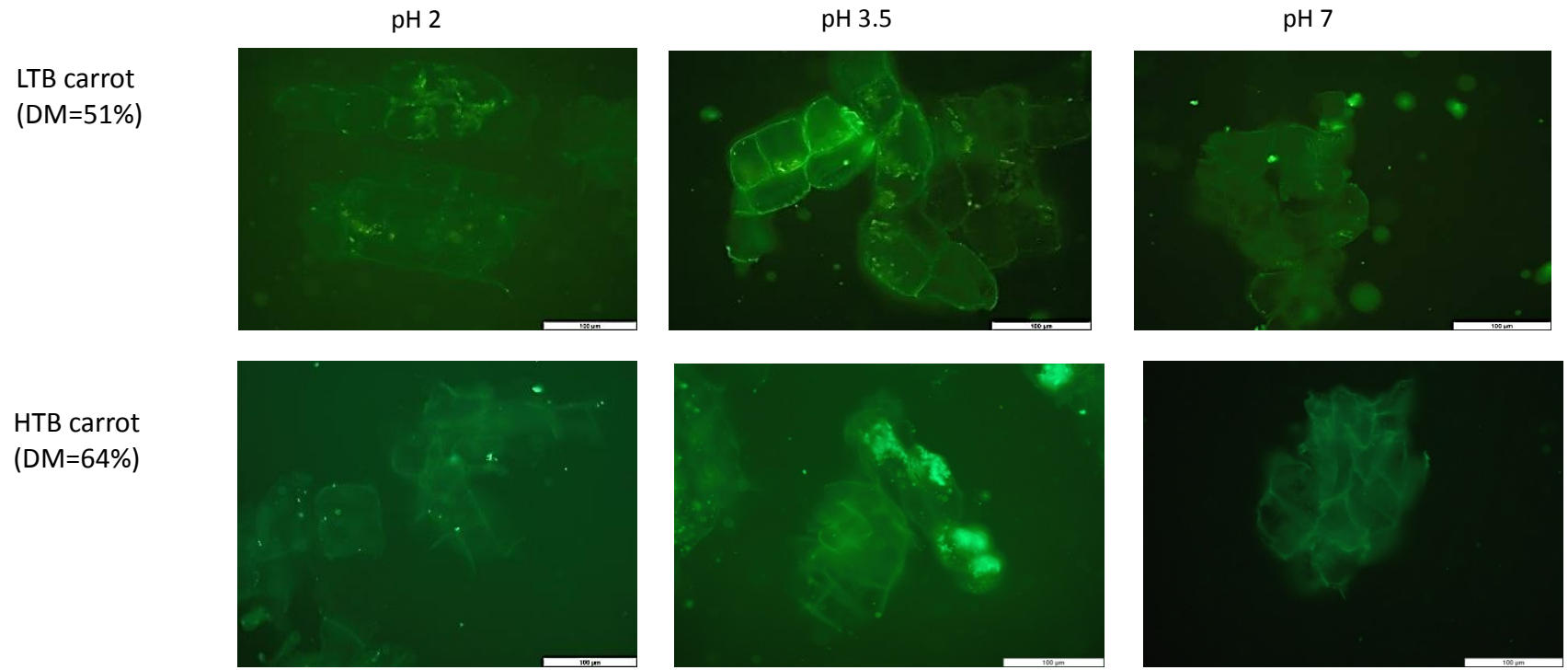

Figure 5

Particle size (µm)	DM (%)	
	LTB	HTB
80-125	51 ± 1	64 ± 1
125-250	49 ± 2	64 ± 1
250-500	42 ± 1	57 ± 1
>500	34 ± 3	54 ± 5
Serum fraction	34 ± 3	76 ± 3

Table 1. Average DM values of pectin present in tissue particles of different sizes and serum fraction obtained from LTB and HTB carrot purées with the associated standard deviations (± SD).

Supplementary Data

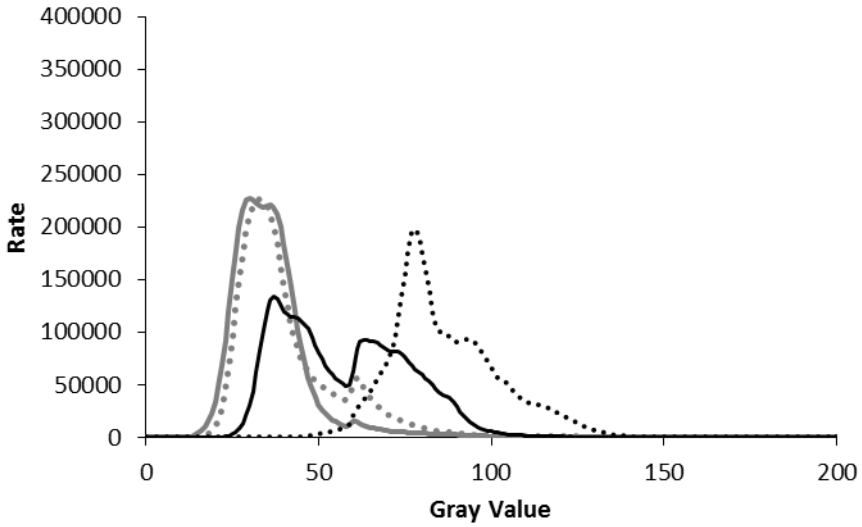

Supplementary Figure 1. Intensity maps of representative images of Ca^{2+} mediated pectin-pectin interactions between fluorescently labeled pectin (DM 16%) and pectin at the surface of HTB carrot particles. —and ····· represent intensities of particles of 80-125 µm (DM 64%) suspended in water without and with 0.1 M $CaCl_2$, respectively. ····and represent intensities of particles of > 500 µm (DM 54%) suspended in water without and with 0.1 M $CaCl_2$, respectively. The gray value increases with decreasing DM of particles and increasing calcium concentration. Similar trends were exhibited in presence of labeled pectin (DM 35, 66% and 95%) (results not shown).

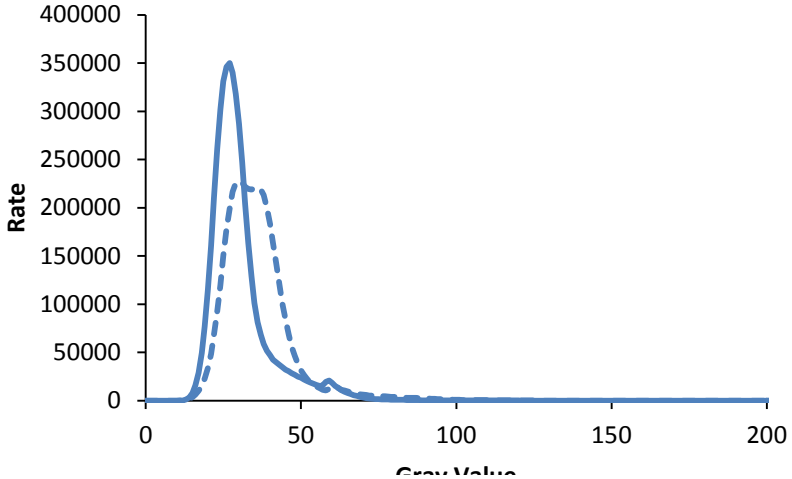

Supplementary Figure 2. Intensity maps of representative images of Ca^{2+} mediated pectin-pectin interactions between fluorescently labeled pectin (DM 16%) and pectin at surface of HTB carrot particles. - - and —— represent intensities of particles of 80-125 µm (DM 64%) suspended in water and carrot serum, respectively. A higher gray value was obtained when the particles

were suspended in water compared to when suspended in serum pectin. Similar trends were obtained for results not shown.

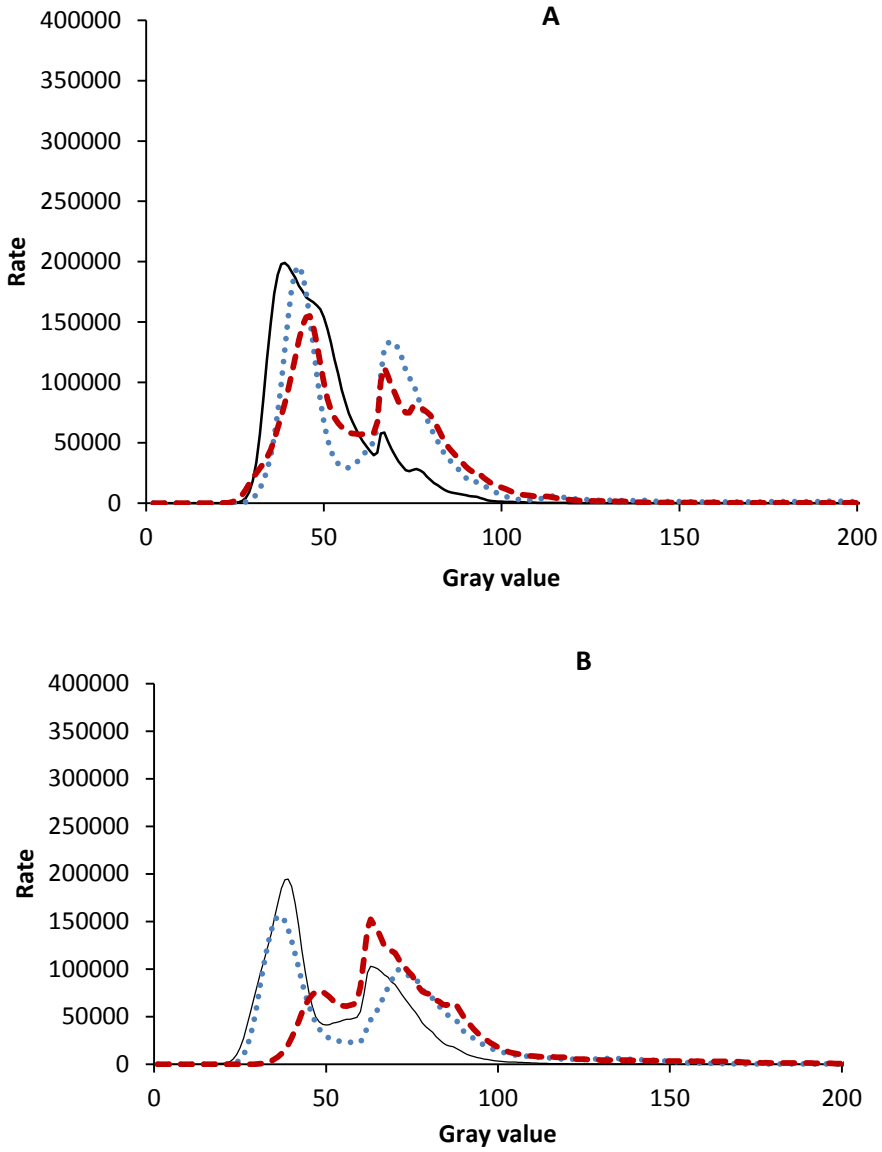

Supplementary Figure 3. Intensity maps of representative images of Ca^{2+} mediated pectin-pectin interactions between fluorescently labeled pectin (DM 16%) and pectin at surface of carrot particles suspended in water at different pHs in presence of 0.1 M $CaCl_2$. (A) and (B) show intensities maps of 80-125 µm particles from LTB and HTB carrots, respectively. —— , ... and - - - represent pH 2, 3.5 and 7, respectively. In both case, the gray value increased with pH. Similar trends were exhibited by >500µm particles (results not shown).